

Supporting Information

Natural Killer T Cell Nanoagonists for Synergistic Immunotherapy of Hepatocellular Carcinoma

Ting Luo[†], Xiaoqiong Tan[†], Guangchao Qing, Jie Yu^{*}, Xing-Jie Liang^{*}, and Ping Liang^{*}

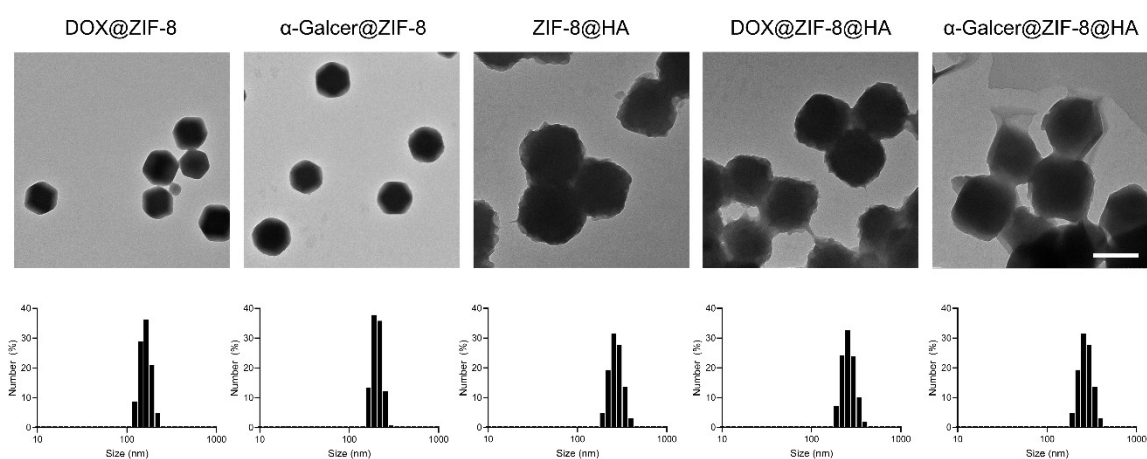


Figure S1. TEM images and hydrodynamic diameters of DOX@ZIF-8, α -Galcer@ZIF-8, ZIF-8@HA, DOX@ZIF-8@HA, and α -Galcer@ZIF-8@HA NPs. Scale bar, 200 nm.

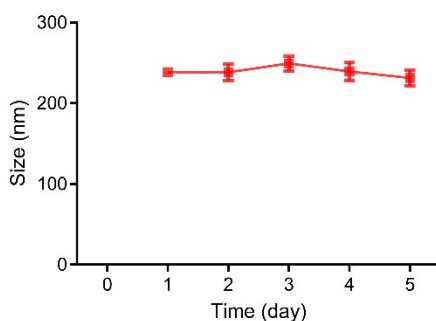


Figure S2. Hydrodynamic diameters of α -Galcer@ZIF-8@HA NPs in DMEM medium during five days.

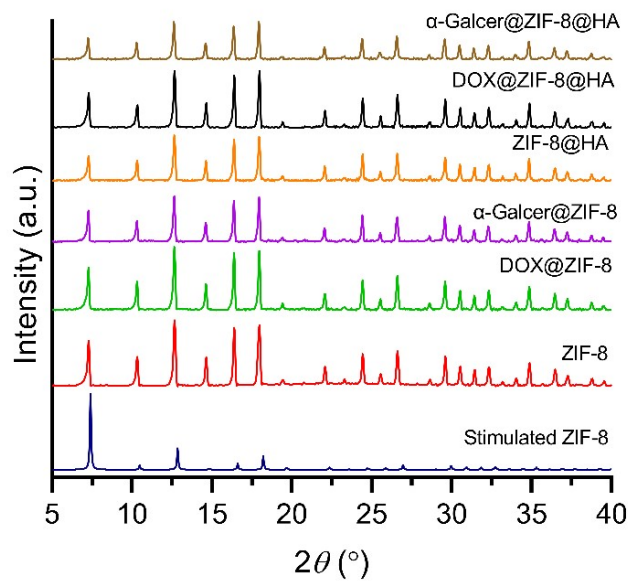


Figure S3. XRD patterns of ZIF-8, DOX@ZIF-8, α -Galcer@ZIF-8, ZIF-8@HA, DOX@ZIF-8@HA, and α -Galcer@ZIF-8@HA NPs.

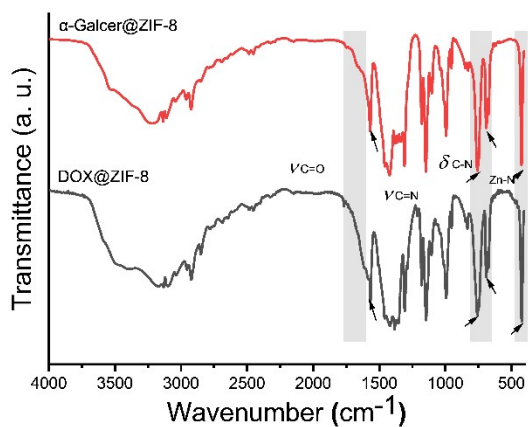


Figure S4. FT-IR spectra of α -Galcer@ZIF-8 and DOX@ZIF-8 NPs.

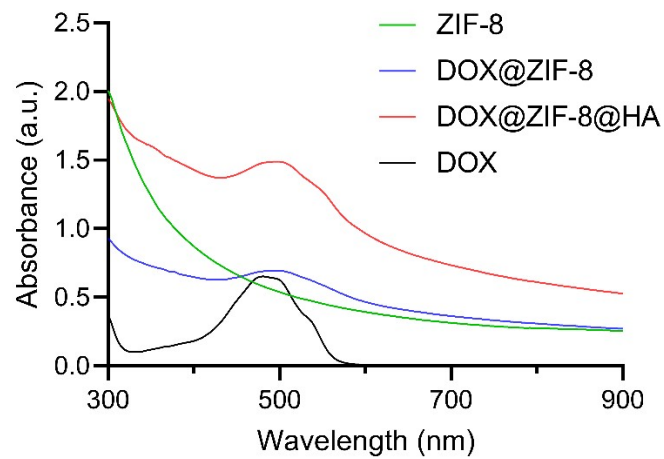


Figure S5. UV-Vis absorption curves of free DOX, ZIF-8, DOX@ZIF-8, and DOX@ZIF-8@HA.

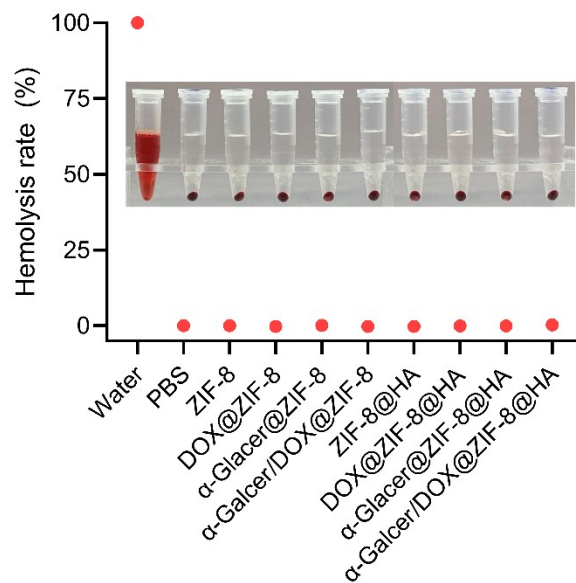


Figure S6. Hemolytic analysis of red blood cells exposed to different formulations.

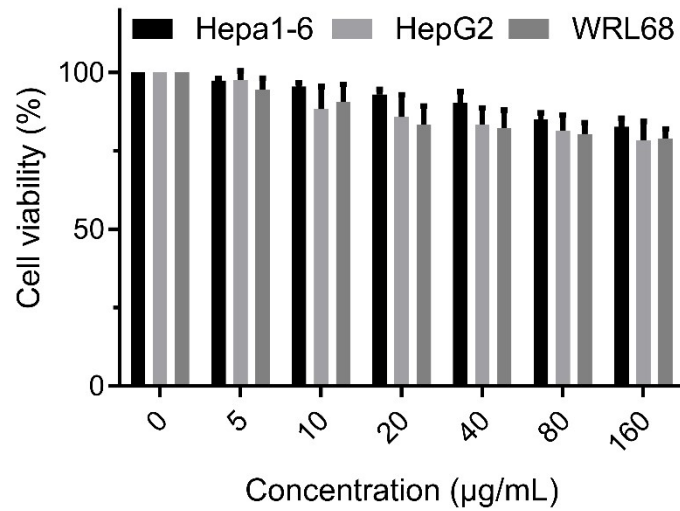


Figure S7. Cell viabilities of Hepa1-6, HepG2, and WRL68 cells treated with ZIF-8 of different concentrations for 24 h (n = 3).

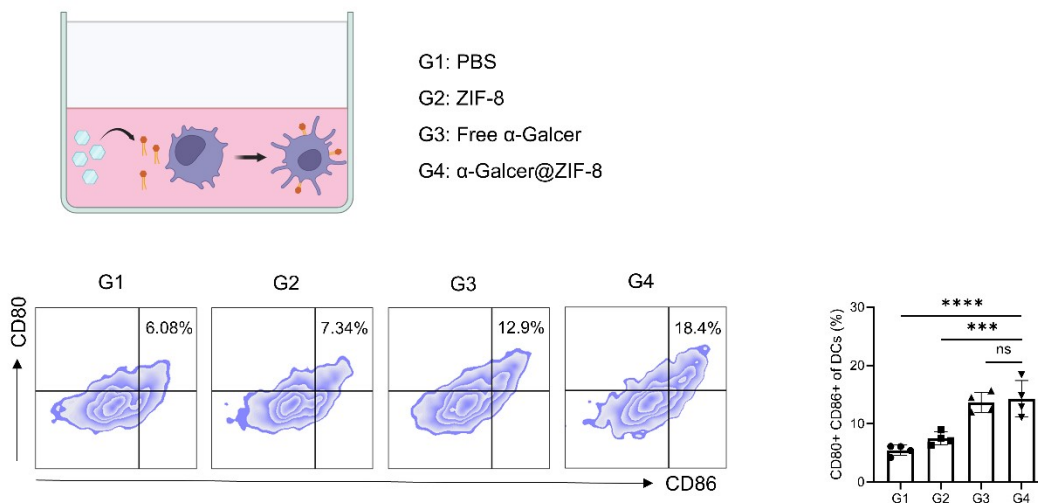


Figure S8. Flow cytometry and quantification analysis of BMDC maturation as triggered by the α -Galcer@ZIF-8 nanoparticles (n = 4). One-way ANOVA with Dunnett's multiple comparison was used to calculate statistical differences. * p < 0.05; ** p < 0.01; *** p < 0.001; **** p < 0.0001.

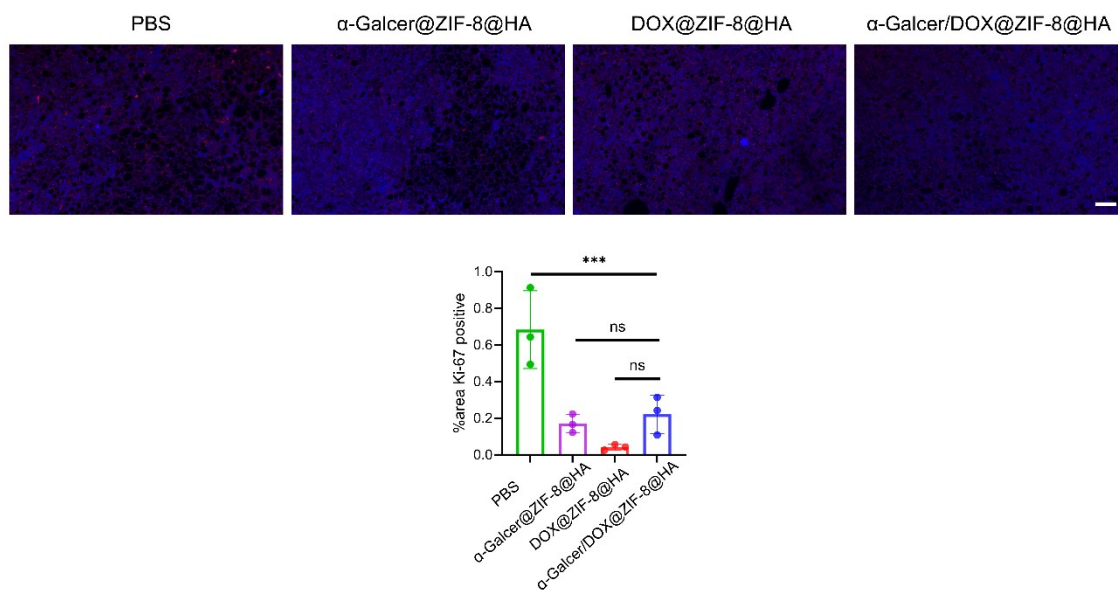


Figure S9. Ki-67 staining and its quantification of Hepa1-6 tumor (n = 3). One-way ANOVA with Dunnett's multiple comparison was used to calculate statistical differences. * p < 0.05; ** p < 0.01; *** p < 0.001; **** p < 0.0001. Scale bar, 100 μm.

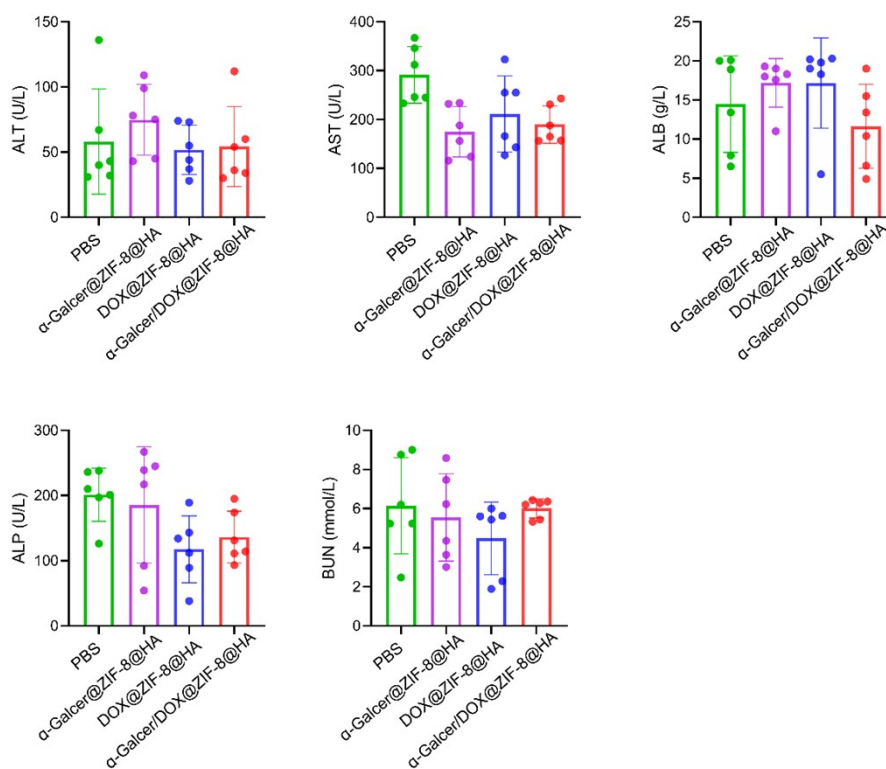


Figure S10. Blood biochemistry analysis in Hepa1-6 tumor bearing mice (n = 6).

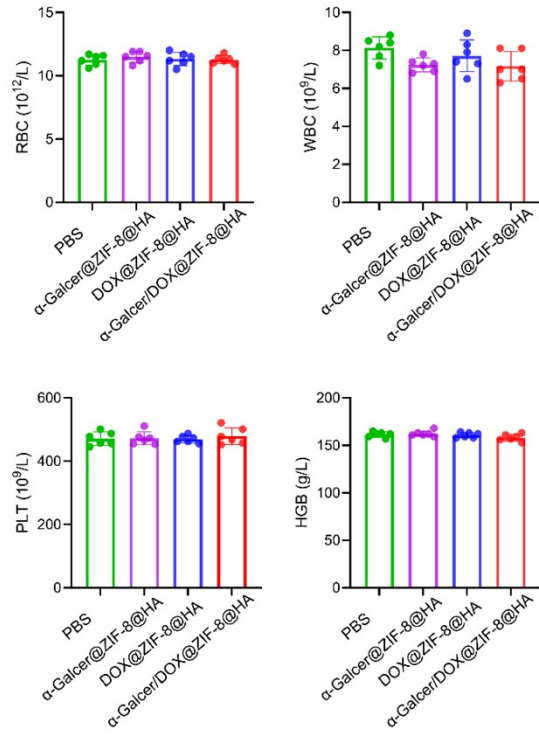


Figure S11. Blood routine analysis in Hepa1-6 tumor bearing mice (n = 6).

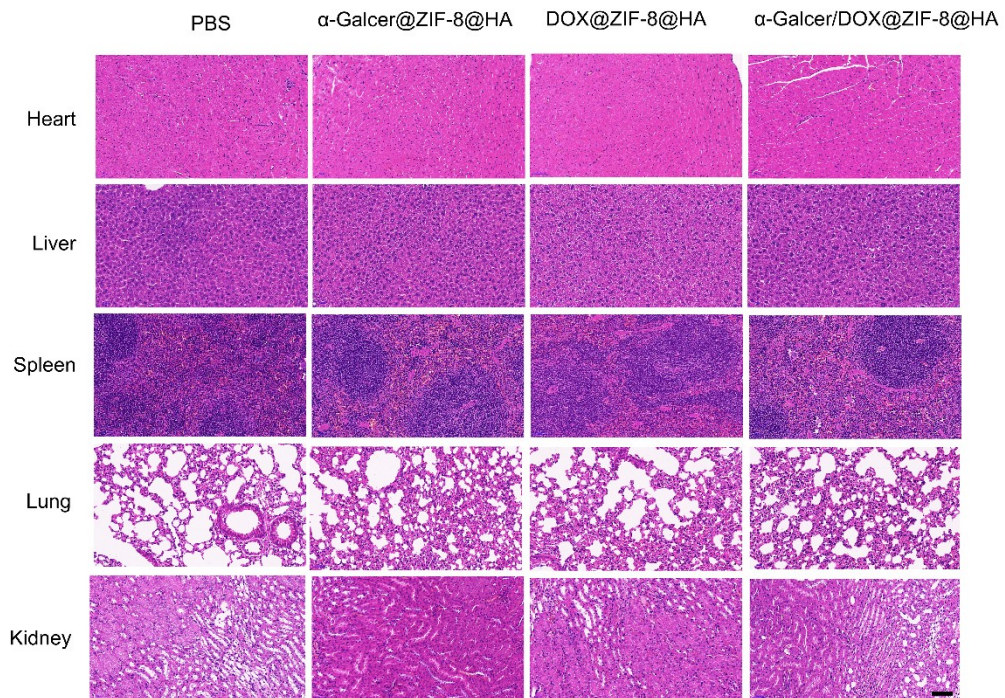


Figure S12. H&E staining of organs in Hepa1-6 tumor bearing mice. Scale bar, 100 μ m.

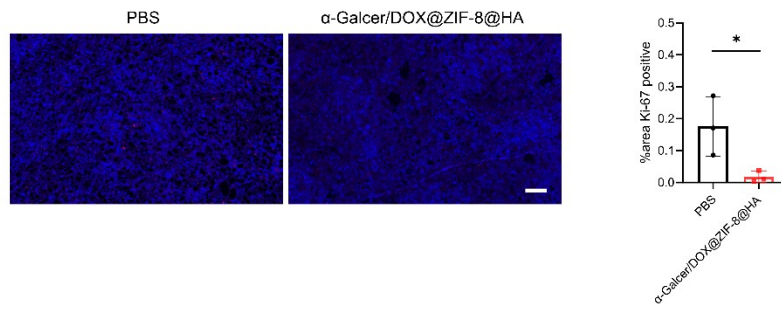


Figure S13. Ki-67 staining and its quantification of DEN-CCl₄ induced orthotopic liver tumor (n = 3). * p < 0.05; ** p < 0.01; *** p < 0.001; **** p < 0.0001, calculated by two-tailed unpaired Student t-test. Scale bar, 100 μm.

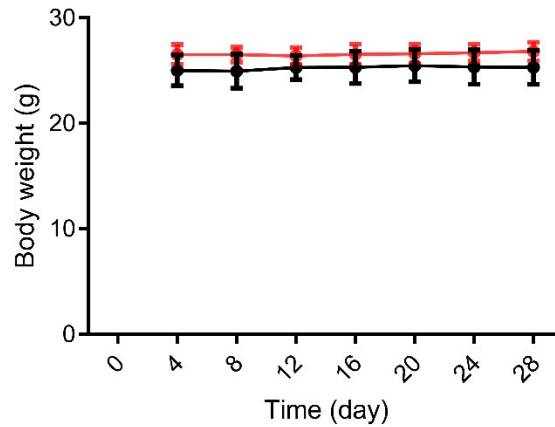


Figure S14. Body weight changes of DEN-CCl₄ induced orthotopic liver tumor bearing mice (n = 5).

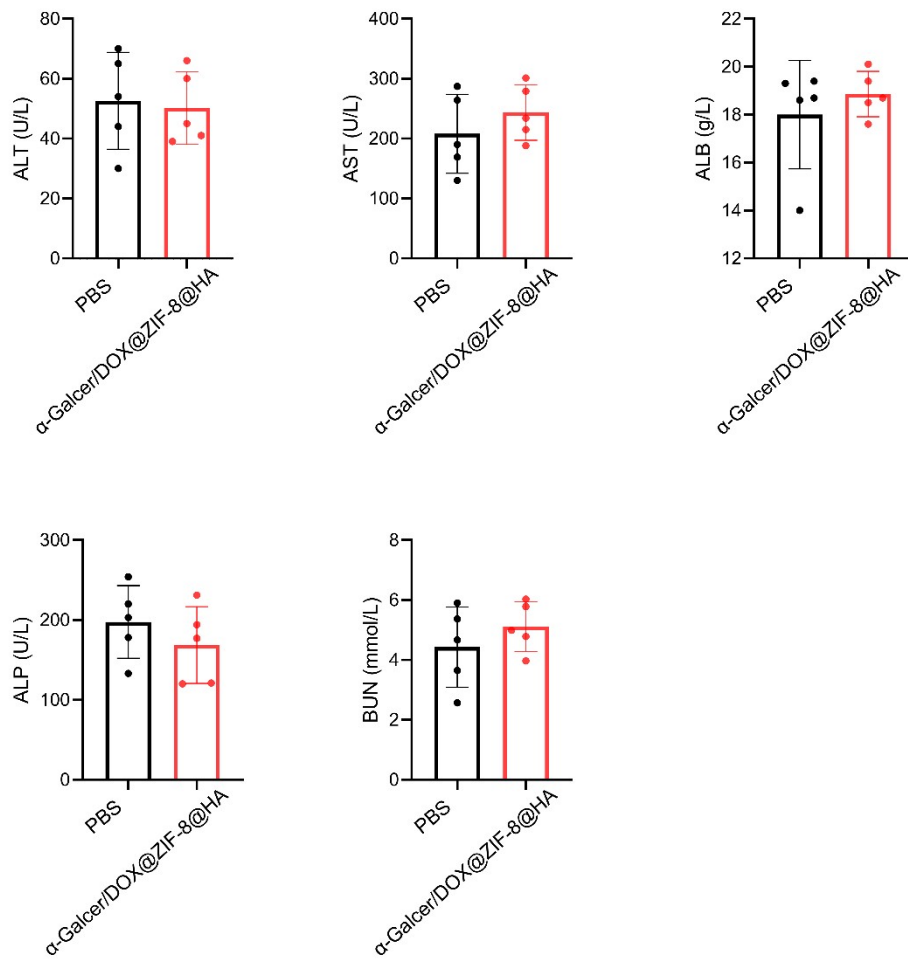


Figure S15. Blood biochemistry analysis in DEN-CCl₄ induced orthotopic liver tumor bearing mice (n = 5).

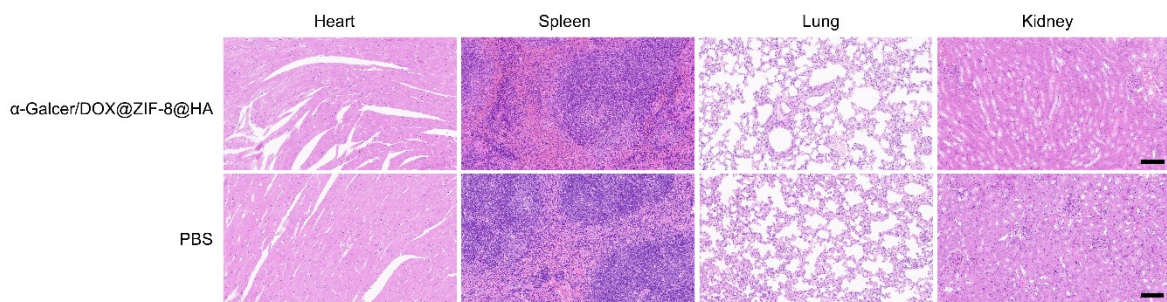


Figure S16. H&E staining of organs in DEN-CCl₄ induced orthotopic liver tumor bearing mice. Scale bar, 100 μ m.

Table S1. Drug loading efficiency

NPs	LE _{DOX} (%)	LE _{α-Galcer} (%)
DOX@ZIF8	8.83	-
α -Galcer@ZIF8	-	0.56
DOX/ α -Galcer@ZIF8	7.02	0.47